Since stopped-flow titrations show the heme Fe(III):oxidant ratio to be the same for both oxidants (2.2:1), it is clear that only one oxygen of a $C_6H_5I(OAc)_2$ molecule is used in intermediate formation. The respective k_m terms, therefore, indicate the reactivity of iodobenzene diacetate toward monomeric dfh to be about twice that of iodosobenzene. It seems likely that this may reflect a statistical factor arising from the diacetate having two equivalent oxygen atoms for potential donation to the heme iron center. If such is the case, there appears to be little discrimination between the substrates with respect to attack of heme Fe(III) at C_6H_5I-bound oxygen.

As shown in Table I, the rate of intermediate formation from heme and C_6H_5IO is independent of $[H^+]$ in the region pH 7.1–9.6. This contrasts with the oxidation of dfh by ClO_2^-, wherein rates diminish with increasing alkalinity in the same region, and by H_2O_2, in which a first-order dependence on OH^- is observed. In the dfh–ClO_2^- system, the observed pH dependence may be due to the importance of chlorous acid as an oxidizing substrate; however, this remains speculative. The hydroxide ion dependence of heme oxidation by H_2O_2 has been attributed to HO_2^- serving as the active form of the oxidant, and rate enhancement in the H_2O_2–dfh system observed in phosphate buffers has been suggested to be due to $H_2PO_4^-$ facilitating decomposition of a heme–HO_2^- complex to the "FeO" structure.[2] Similar acid–base ionization is not possible in iodosobenzene, and the absence of a pH effect here offers additional indirect support for the contention that intermediate formation from dfh and H_2O_2 does indeed proceed via attack of heme by oxidant conjugate base, i.e., perhydroxyl anion.[2]

Acknowledgment. This research was supported by The Robert A. Welch Foundation (Grant P-162).

Registry No. Iodosobenzene, 536-80-1; iodobenzene diacetate, 29733-61-7; dfh, 21007-21-6.

Contribution from the Department of Chemistry, Florida State University, Tallahassee, Florida 32306

Oxidative Electrochemistry of Iron Thiocarbonyl Porphyrins

LAWRENCE A. BOTTOMLEY,*[1] MARK R. DEAKIN, and JEAN-NOEL GORCE

Received August 24, 1983

The oxidative electrochemistry of thiocarbonyl(5,10,15,20-tetraphenylporphinato)iron(II), (TPP)FeCS, was studied in 1,2-dichloroethane solution at a Pt-button electrode. Results from detailed voltammetric and combined electronic, IR, and EPR spectroelectrochemical experiments indicated that (TPP)FeCS can be oxidized in two chemically reversible, one-electron transfers. This is in marked contrast with the analogous carbon monoxide Fe(II) porphyrin derivative that loses CO concomitantly with the removal of the first electron. The product of the first oxidation is a thiocarbonyl Fe(III) porphyrin whereas the second oxidation step occurs at the periphery of the porphyrin ring, producing a thiocarbonyl Fe(III) porphyrin radical. Addition of nitrogenous bases to solution generated the monoadduct (TPP)FeCS[nitrogenous base]. This adduct was also oxidized in two discrete, one-electron transfers. The product of the first oxidation, $\{(TPP)Fe^{III}CS$-[nitrogenous base]$\}^+$, was stable for hours. The product of the second oxidation, however, readily underwent nucleophilic attack by uncomplexed nitrogenous base present in solution. The electronic effects generated by the ligand trans to the thiocarbonyl moiety are discussed in the context of their influence on the spectral, electrochemical, and thermodynamic properties of the thiocarbonyliron porphyrin.

Introduction

Synthetic iron porphyrin complexes possessing an iron–carbon bond have received considerable attention recently. The impetus has been provided by the discovery of cytochrome P-450 complexes possessing this bonding moiety.[2] These complexes were formed during the metabolic reduction of polyhalogenated compounds. Such compounds have found widespread use as industrial solvents and as toxic components in fungicide and insecticide formulations. A detailed knowledge of the redox stability of the iron–carbon bond is essential for a complete understanding of this particular aspect of the biochemistry of cytochrome P-450.

Three approaches for preparing synthetic Fe porphyrin compounds with an Fe–C bond have been developed: (1) the direct reaction of Fe porphyrins with isocyanides; (2) the reaction of Fe(I) porphyrins with alkyl halides to form (σ-alkyl)porphyrins; (3) the reaction of either Fe(III) or Fe(II) porphyrins with polyhalogenated compounds under reducing conditions to form iron carbene complexes. The first two schemes have been known for sometime.[3,4] Lexa and co-workers[5] have investigated the electroreduction of the (σ-alkyl)porphyrins in detail. Elliott and Marrese[6] have exploited the second reaction sequence and demonstrated its utility in electrocatalysis. The third reaction scheme has been extensively explored by Mansuy and co-workers.[7]

A particularly intriguing carbene ligand is thiocarbonyl. Relatively few complexes of this type are known, due to the instability of C≡S. The synthetic routes to these complexes have involved either the reduction of thiophosgene or the

(1) To whom correspondence should be addressed at: School of Chemistry, Georgia Institute of Technology, Atlanta, GA 30332.

(2) (a) Wolf, C. R.; Mansuy, D.; Nastainczyk, N.; Deutschmann, G.; Ullrich, V. *Mol. Pharmacol.* **1977**, *13*, 698. (b) Arh, H. J.; King, L. J.; Nastainczyk, W.; Ullrich, V. *Biochem. Pharmacol.* **1982**, *31*, 383.

(3) Caughey, W. S.; Barlow, C. H.; O'Keefe, D. H.; O'Toole, M. C. *Ann. N.Y. Acad. Sci.* **1973**, *206*, 296.

(4) Wade, R. S.; Castro, C. E. *J. Am. Chem. Soc.* **1973**, *95*, 231.

(5) (a) Lexa, D.; Mispelter, J.; Saveant, J.-M. *J. Am. Chem. Soc.* **1981**, *103*, 6806. (b) Lexa, D.; Saveant, J.-M. *Ibid.* **1982**, *104*, 3503. (c) Lexa, D.; Momenteau, M.; Mispelter, J. *Biochim. Biophys. Acta* **1974**, *338*, 151.

(6) Elliott, C. M.; Marrese, C. A. *J. Electroanal. Chem. Interfacial Electrochem.* **1981**, *19*, 395.

(7) (a) Mansuy, D.; Lange, M.; Chottard, J. C.; Guerin, P.; Morliere, P.; Brault, D.; Rougee, M. *J. Chem. Soc., Chem. Commun.* **1977**, 648. (b) Mansuy, D.; Lange, M.; Chottard, J. C.; Bartolia, J. F.; Chevrier, B.; Weiss, R. *Angew. Chem., Int. Ed. Engl.* **1978**, *17*, 781. (c) Mansuy, D. *Pure Appl. Chem.* **1980**, *7*, 215. (d) Mansuy, D.; Guerin, P.; Chottard, J. C. *J. Organomet. Chem.* **1979**, *171*, 195. (e) Guerin, P.; Battioni, J. P.; Chottard, J. C. *J. Organomet. Chem.* **1981**, *218*, 201. (f) Mansuy, D.; Battioni, J. P.; Chottard, J. C.; Ullrich, V. *J. Am. Chem. Soc.* **1979**, *101*, 3971. (g) Mansuy, D.; Lange, M.; Chottard, J. C. *J. Am. Chem. Soc.* **1978**, *100*, 3213. (h) Mansuy, D.; Lecomte, J. P. Chottard, J. C.; Bartoli, J. F. *Inorg. Chem.* **1981**, *20*, 3119.

0020-1669/84/1323-3563$01.50/0

desulfurization of coordinated CS_2.[8] Recently, thiocarbonyl complexes of metalloporphyrins (where the central metal was Fe,[9,11] Ru,[10] and Os[11]) have been reported. Mansuy and co-workers[9] reported that the Fe–C bond is particularly unreactive toward nucleophiles, as compared to other carbene Fe porphyrins. In the presence of a 20 000-fold excess of pyridine, less than 5% of (TPP)FeCS[12] had decomposed after a 24-h period. This complex is also remarkably stable toward O_2, permitting the ready isolation of this Fe(II) porphyrin in air.

The reductive electrochemistry of carbene Fe porphyrins has been examined.[13,14] The successive injection of two electrons into these complexes triggers chemical reactions essentially involving the carbene moiety. For example, electroreduction of (TPP)FeCS in DMF yields a thiocarbonyl Fe(II) porphyrin dianion that readily adds a proton to form the thioformyl Fe(II) porphyrin anion.

The oxidative electrochemistry of carbene Fe porphyrins has not been extensively investigated. Mansuy[9] has reported the dissociation of the Fe–C bond when (TPP)FeCS is treated with one-electron oxidants such as ferric chloride. However, Buchler and co-workers[11] have observed a reversible one-electron oxidation of both (OEP)FeCS and (TPP)FeCS by cyclic voltammetry. This observation is particularly fascinating in the context of similar studies on the C≡O complexes of Fe porphyrins. Oxidation of O=C—Fe porphyrins occurs concomitantly with the dissociation of the Fe—C bond.[15,16]

The aim of the research reported herein was the resolution of the apparent contradiction provided by the results of the electrochemical vs. chemical oxidation of (TPP)FeCS. With a number of voltammetric and combined spectroscopic–electrochemical methods, the electrooxidation of (TPP)FeCS and various nitrogenous base adducts of (TPP)FeCS has been investigated. An electron-transfer mechanism is proposed, consistent with all of the observed results.

Experimental Section

Materials. The synthesis of thiocarbonyl(5,10,15,20-tetraphenylporphinato)iron(II), (TPP)FeCS, was accomplished via a modification of the method of Buchler and co-workers[11] in their preparation of the thiocarbonyl adduct of iron(II) octaethylporphyrin. In a typical preparation of (TPP)FeCS, 700 mg of $[(TPP)Fe]_2O$ (previously prepared by the method of Adler and co-workers[17]) was dissolved in 100 mL of CH_2Cl_2 and extracted twice with equal volumes of 2 M HCl. The organic layer was dried over anhydrous Na_2SO_4 and then reduced to dryness on a rotary evaporator. The solid was dissolved in 75 mL of tetrahydrofuran, that had been previously distilled under N_2 from sodium benzophenone ketal. The solution was transferred to a 200-mL Schlenk pot and deoxygenated by three freeze–pump–thaw cycles. Approximately 10 mL of a 1.0% Na/Hg amalgam was added to the flask under an N_2 atmosphere. The mixture was stirred for 5 min with no perceptible color change. Then, 1.75 mL of thiophosgene (Aldrich Chemicals) was injected via syringe through a septum into the reaction mixture. Over the next 15 min, a fine white suspension developed. The mixture was stirred for 3 h, filtered, and then reduced to dryness on a rotary evaporator. The crude product was dissolved in a minimum volume of benzene and applied to a column of neutral alumina. Elution with 3:2 (v/v) mixture of CH_2Cl_2/benzene afforded first a bright red band that rapidly eluted and a slow-moving green band. The first band was collected and spectrally characterized as (TPP)FeCS. The visible and infrared spectra were in agreement with that previously published by Mansuy and co-workers[9] for this compound.

All nitrogenous bases were purchased and used as received from Aldrich Chemical Co. The supporting electrolyte, tetrabutylammonium perchlorate, TBAP, was obtained from the Eastman Chemical Co. Prior to use, TBAP was recrystallized three times from absolute ethanol, vacuum dried for 24 h, and stored in a evacuated desiccator. 1,2-Dichloroethane[12] was extracted successively from concentrated sulfuric acid and distilled water. The resultant extract was fractionally distilled over phosphorus pentoxide in a nitrogen atmosphere and stored in the dark over activated 4-Å molecular sieves.

Instrumentation. Visible spectral measurements were obtained with a Tracor Northern optical multichannel analysis system. The system was composed of a Tracor Northern 6050 spectrometer containing a crossed Czerny–Turner spectrograph in conjunction with the Tracor Northern 1710 multichannel analyzer. Spectra were acquired by irradiation of the sample with polychromatic light from a tungsten–halogen source and the subsequent spatial dispersion of the transmitted radiation onto the detector, a linear 512 diode array by a grating with a 300 g/mm rule and a blaze of 520 nm. In the first order, this provided spectral resolution of 0.6 nm per diode. The LSI-11 minicomputer processed the spectral data and stored the complete spectral band (from 360 to 670 nm) in memory. Wavelength calibration was achieved with a holmium oxide filter. All measurements reported herein represent the ensemble average of at least 128 spectral acquistions. For display purposes, a five-point Savitsky–Golay smoothing algorithm was applied to the spectra prior to output onto a Houston Omnigraphic 2000 X-Y recorder. Spectrophotometric titrations were carried out in a 1.00-cm path length quartz cuvette.

Cyclic voltammetric experiments (CV) were carried out with either an EG&G Princeton Applied Research Model 174A polarographic analyzer or an IBM Instruments, Inc., Model EC225 polarographic system. A conventional three-electrode system was used with a Pt-button working electrode, a Pt-wire counterelectrode, and a saturated calomel electrode as reference, SCE. Aqueous contamination of electrochemical solutions from the references electrode fill solution was minimized by isolating the reference electrode via a frit. Voltammograms were recorded on a Houston Omnigraphic 2000 X-Y recorder. Scan rates ranged from 20 to 1000 mV/s for cyclic voltammetric experiments. To compensate for solution resistance, positive-feedback *ir* compensation was employed when measurements were made with the IBM Instruments, Inc., Model E225 polarographic system.

Differential-pulse voltammetric (DPV) experiments were performed with the equipment listed above except that both instruments were modified to allow the user to select the pulse direction independently of the potential sweep direction.[18,19] For all DPV experiments, a potential scan rate of 10 mV/s was employed. Pulse intervals varied between 0.1 and 0.5 s while pulse amplitudes varied between 10 and 110 mV.

All solutions were deoxygenated by passing a stream of solvent-saturated prepurified N_2 into the solution for at least 10 min prior to recording voltammetric data. To maintain an O_2-free environment, the solution was blanketed with N_2 during all experiments. All potentials reported herein were referenced to the SCE and were uncorrected for liquid-junction potentials. The uncertainty in each potential reported herein (except where noted otherwise) is ±10 mV.

Spectroelectrochemical experiments were performed in an optically transparent thin-layer electrochemical cell with an optical path length of 0.15 mm. The cell design was a modification of that previously presented by Lexa and co-workers.[20] The working electrode consisted of an easily removable Pt-gauze electrode of 0.49-cm^2 active area. The counterelectrode was a Pt wire coiled to minimize its physical dimensions. The reference electrode was that used for voltammetry.

(8) (a) Butler, I. S.; Fenster, A. E. *J. Organomet. Chem.* **1974**, *66*, 161. (b) Yaneff, P. V. *Coord. Chem. Rev.* **1977**, *23*, 183. (c) Butler, I. S. *Acc. Chem. Res.* **1977**, *10*, 359.
(9) (a) Battioni, J.-P.; Chottard, J.-C.; Mansuy, D. *J. Am. Chem. Soc.* **1978**, *100*, 4311. (b) Battioni, J.-P.; Chottard, J.-C.; Mansuy, D. *Inorg. Chem.* **1982**, *21*, 2056.
(10) Smith, P. D.; Dolphin, D.; James, B. R. *J. Organomet. Chem.* **1981**, *208*, 239.
(11) Buchler, J. K.; Kobisch, W.; Smith, P. D.; Tonn, B. *Z. Naturforsch., B: Anorg. Chem., Org. Chem.* **1978**, *33B*, 1371.
(12) Abbreviations: L = ligand; TPP = 5,10,15,20-tetraphenylporphinato dianion; OEP = octaethylporphinato dianion; $EtCl_2$ = 1,2-dichloroethane.
(13) Lexa, D.; Saveant, J.-M.; Battioni, J.-P.; Lange, M.; Mansuy, D. *Angew. Chem., Int. Ed. Engl.* **1981**, *20*, 578.
(14) Battioni, J.-P.; Lexa, D.; Mansuy, D.; Saveant, J.-M. *J. Am. Chem. Soc.* **1983**, *105*, 207.
(15) Brown, G. M.; Hopf, F. R.; Meyer, T. J.; Whitten, D. G. *J. Am. Chem. Soc.* **1975**, *97*, 5385.
(16) Gurira, R. C.; Jordan, J. *Anal. Chem.* **1981**, *53*, 864.
(17) Adler, A. D.; Longo, F. R.; Kampas, F.; Kim, K. *J. Inorg. Nucl. Chem.* **1970**, *32*, 2443.
(18) Birke, R. L.; Kim, M.-H.; Strassfeld, M. *Anal. Chem.* **1981**, *53*, 852.
(19) Bottomley, L. A.; Deakin, M. R., manuscript in preparation.
(20) Lexa, D.; Saveant, J.-M.; Zickler, J. *J. Am. Chem. Soc.* **1977**, *99*, 2786.

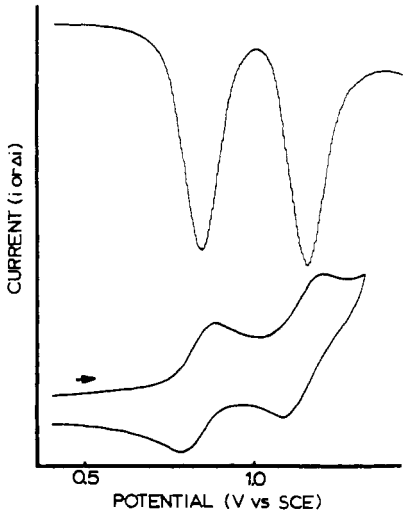

Figure 1. Voltammetric data obtained during the electrooxidation of (TPP)FeCS in $EtCl_2$ containing 0.1 M TBAP. The upper trace is the differential-pulse voltammogram obtained at a Pt-button electrode with a potential sweep rate of 10 mV s^{-1}, a pulse interval of 0.5 s, and a pulse amplitude of 25 mV. The lower trace is the cyclic voltammogram obtained with a potential sweep rate of 200 mV s^{-1}.

Potentials for the spectroelectrochemical measurements were regulated by an EG&G Princeton Applied Research Model 173D potentiostat/galvanostat and a Krohn-Hite Model 5200A function generator.

Infrared spectroscopy was performed on a Perkin-Elmer 983 IR spectrometer using NaCl solution cells. Unless otherwise noted, the solvent was $CHCl_3$ for these measurements. EPR data were gathered at X-band with a Varian E-12 spectrometer. Magnetic field strengths were accurately measured with a Spectromagnetic Industries Model 520 NMR gaussmeter.

Methods. Spectrophotometric titrations were carried out in the conventional manner using Hamilton Microliter syringes for transferring aliquots of titrant into the analyte solution. The titrant consisted of (TPP)FeCS, identical in concentration to that of the analyte, as well as a large excess of ligand. No displacement of the thiocarbonyl moiety by the nitrogeneous base was observed, even in the presence of a 1000-fold excess of the strongest base utilized. The spectral data were analyzed by the method of Benesi and Hildebrand.[21] Titrations monitored with differential-pulse voltammetry were performed in the manner previously described.[22] Formation constants were computed from electrochemical data in the usual fashion.[23]

Results

Voltammetric Characterization of (TPP)FeCS. Two separate electron-transfer processes were observed during the electrooxidation of (TPP)FeCS in $EtCl_2$ solution. Typical cyclic and differential-pulse voltammograms are depicted in Figure 1. Analysis of the cyclic voltammetric data obtained for the first oxidation process over the potential sweep rate range of 20–1000 mV s^{-1} indicated that the half-wave potential (measured at 850 ± 5 mV) was independent of potential sweep rate. The ratio of the cathodic to anodic peak currents was essentially 1. The ratio of the anodic peak current over the square root of the potential sweep rate decreased in a nonlinear fashion with increasing potential sweep rate. At 20 mV s^{-1}, the anodic to cathodic peak potential separation was 63 ± 1 mV and increased with increasing sweep rate.

The first oxidation process was also analyzed by differential-pulse voltammetry as per the method of Birke.[18] The peak currents obtained with positive potential pulses superimposed on a linear potential ramp were equal to the peak currents

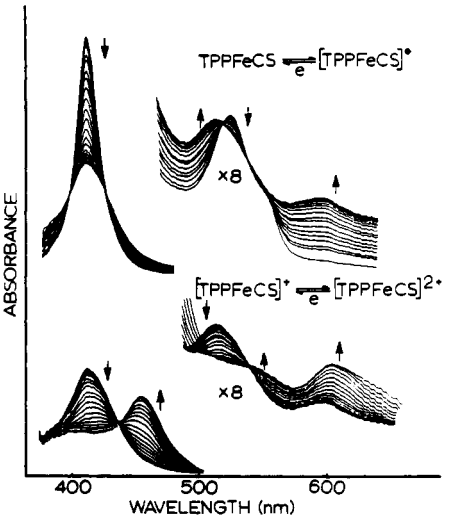

Figure 2. Spectra obtained during the incremental potential-step experiment on a solution of 0.292 mM (TPP)FeCS in $EtCl_2$ over the potential region 0.72–1.02 V (upper portion) and 1.02–1.21 V (lower portion).

obtained with a negative pulse. At a pulse amplitude of 10 mV, the peak width at half-height was 100 ± 2 mV (as compared to the theoretical value of 90.4 mV for a reversible one-electron transfer) and increased with increasing pulse amplitude. Variation of the pulse amplitude from 10 to 110 mV yielded peak potential separation $[E_{p(+)} - E_{p(-)}]$ values within 1 mV of the pulse ampltiude. Taken collectively, the voltammetric data indicated that the first oxidation process was best described as a quasi-reversible, one-electron transfer. The chemical reversibility of this process was confirmed coulometrically. Chronocoulometric experiments were employed to obtain the measurement of the diffusion coefficient for (TPP)FeCS as 8.9 (±0.3) × 10^{-6} cm^2 s^{-1}. With this value and the conventional cyclic voltammetric data analysis method,[24] the heterogeneous rate of electron transfer was computed as 3.6 (±0.5) × 10^{-2} cm s^{-1}. This value resides within the boundary zone suggested by Matsuda and Ayabe[25] for a quasi-reversible electron transfer.

Cyclic and differential-pulse voltammetric experiments and data analyses identical with those described above for the first oxidation process were performed on the second oxidation process, with comparable results. This process, occuring at 1160 ± mV, is also best described as a quasi-reversible, one-electron transfer.

Spectroelectrochemical Characterization of (TPP)FeCS. The stepwise oxidation of (TPP)FeCS was monitored spectrally via electrolysis at controlled potential in an optically transparent electrochemical cell. The interconversion of (TPP)FeCS to its first and second oxidized products was investigated by an incremental, small-potential-step experiment previously described by Su and Heineman.[26] Between the potential of zero current (0.13 V) and 0.72 V, no spectral changes occurred. From this point, the potential was increased in 10-mV increments and the system was allowed to stabilize for 3 min prior to the spectral acquisition. Spectral changes were ~95% complete within 10 s of potential application. Over the potential region of 0.72–0.94 V, a sizable decrease in the intensity of the Soret band (~50%) was observed as a function of potential. Similarly, the α band shifted toward the red by 48 nm, and the β band shifted toward the blue by 12 nm, also as a function of the applied potential. The spectra

(21) Benesi, H. A.; Hildebrand, J.; *J. Am. Chem. Soc.* **1949**, *71*, 2703.
(22) Bottomley, L. A.; Kadish, K. M. *Anal. Chim. Acta* **1982**, *139*, 367.
(23) Bottomley, L. A.; Olson, L.; Kadish, K. M. In "Electrochemical and Spectroscopic Studies on Biological Redox Components"; Kadish, K. M., Ed.; American Chemical Society: Washington, DC, 1982; Adv. Chem. Ser. No. 201, p 279.
(24) Nicholson, R. S. *Anal. Chem.* **1965**, *37*, 1351.
(25) Matsuda, H.; Ayabe, Y. *Z. Elektrochem.* **1955**, *59*, 494.
(26) Su, C.-H.; Heineman, W. R. *Anal. Chem.* **1981**, *53*, 594.

obtained during this interconversion process are depicted in the upper portion of Figure 2. Note the presence of four neat isosbestic points at 396, 424, 515, and 536 nm, indicating the absence of any long-lived intermediates. Analysis of the spectral absorbance changes as a function of the applied potential (as per the method of Su and Heineman[26]) confirmed the passage of 1 equiv of charge and a formal potential of 0.85 V for the first oxidation process.

Incremental potential steps over the potential region of 0.95–1.02 V yielded no spectral changes. The absence of any slow decomposition products was confirmed by holding the electrode at 1.02 V. After 2 h, the electronic spectrum was unchanged. At open circuit, however, the first oxidation product was stable for only 5 min. After this time period, a gradual enhancement in the Soret band intensity was observed; the Soret band maximum shifted to 411 nm. Simultaneously, the α band dissapeared whereas the β band shifted (toward the red) to 515 nm and lost intensity.

The spectra obtained during the incremental potential step experiment beyond 1.02 V are depicted in the lower portion of Figure 2. The Soret band at 407 nm gradually disappeared while a new band presented itself at 451 nm. Likewise, the β band lost intensity and shifted to 541 nm while the α band gained in intensity and shifted to 602 nm. Isosbestic points appeared at 433 and 525 nm. Analysis of the spectral absorbance changes as a function of applied potential confirmed the passage of 1 equiv of charge, and a formal potential of 1.16 V was measured for the second oxidation process.

A time-resolved thin-layer spectroelectrochemical experiment was carried out on a fresh solution of (TPP)FeCS. The potential was stepped from the potential of zero current to 0.97 V. The spectrum of the first oxidation product was obtained after 50 s. After 1 h, no spectral changes were observed. The potential of the minigrid electrode was then stepped back to 0.13 V, and within 60 s, the spectrum of the starting material was regenerated. Comparison of the Soret band intensities measured initially and after the return of the applied potential to 0.13 V indicated that 99.5% of the starting material had been reversibly electrolyzed.

On a fresh solution of (TPP)FeCS, the first oxidation product was generated (as described above) and then the potential was stepped to 1.28 V. The spectral transformation to that of the second oxidation product was accomplished within 60 s, and isosbestic points were observed at 433, 496, and 525 nm. After 5 min the applied potential was stepped back to 0.97 V, converting the material in the thin-layer cell back to that of the first oxidation product. Comparison of the intensities measured before and after the formation of the second oxidation product indicated that 97% of the starting material had been reversibly electrolyzed. Taken collectively, these results indicated that both electron-transfer reactions were chemically reversible. The first process yielded a product that was stable in the electrolysis cell for the least 2 h. In contrast, the second oxidation product was stable for only ~15 min under the conditions employed.

Spectroscopic Characterization of (TPP)FeCS. The electronic spectrum of (TPP)FeCS dissolved in $EtCl_2$ possessed the spectral characteristics typical of low-spin Fe(II) porphyrins with a Soret band at 407 nm and two visible bands at 522 and 548 nm, respectively. These wavelengths are within 2 nm of those reported by Mansuy et al.[9] for the same material dissolved in benzene. Addition of TBAP into the solution (up to a concentration of 0.2 M) caused no measurable change in the spectrum.

Addition of nitrogenous bases to solution produced significant spectral line shifts with little or no change in the intensities of the spectral lines. Substantial red shifts were observed for all lines; the Soret band shifted from 14 to 17 nm, the α band from 29 to 38 nm, and the β band between 19 to 25 nm, depending upon the identity of the nitrogenous base added to solution. Table I lists the peak maxima and molar absorptivities observed for (TPP)FeCS solutions in the presence of 15 different nitrogeneous bases.

Table I. Spectral Data[a] for (TPP)FeCS[L] Complexes

ligand	electronic spectral features[b]			ν(C=S),[c] cm^{-1}
none	407 (1.92)	522 (0.14)	548 (0.08)	1308
3,5-dichloropyridine	421 (2.04)	541 (0.13)	577 (0.05)	1302
3-cyanopyridine	421 (1.94)	541 (0.12)	577 (0.05)	1300
4-cyanopyridine	421 (2.01)	541 (0.12)	578 (0.05)	1299
3-chloropyridine	421 (1.91)	542 (0.12)	578 (0.05)	1296
3-bromopyridine	421 (1.98)	542 (0.12)	580 (0.07)	1297
3-acetylpyridine	422 (1.93)	543 (0.12)	580 (0.05)	
4-acetylpyridine	422 (1.90)	542 (0.12)	579 (0.06)	
aniline	422 (1.83)	542 (0.12)	580 (0.05)	1296
pyridine	422 (2.03)	542 (0.12)	579 (0.07)	1295
3-picoline	422 (1.89)	543 (0.09)	579 (0.04)	1294
4-picoline	422 (1.88)	543 (0.10)	580 (0.05)	1294
3,4-dimethylpyridine	423 (1.97)	543 (0.10)	580 (0.05)	1293
imidazole	424 (1.82)	546 (0.09)	583 (0.05)	1290
1-methylimidazole	424 (1.80)	547 (0.10)	586 (0.05)	1289
piperidine	424 (1.78)	542 (0.10)	577 (0.04)	1289

[a] Solvent system: $EtCl_2$, 0.1 M in TBAP. [b] Values listed are peak maxima in nm; values in parentheses are the molar absorptivities at peak maximum divided by 10^5. [c] Measurements made in $CHCl_3$.

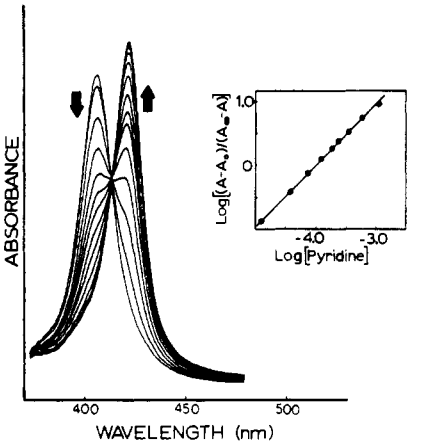

Figure 3. Spectrophotometric data obtained during the titration of a 2.34×10^{-6} M solution of (TPP)FeCS with pyridine. The inset depicts a Benesi–Hildebrand plot providing analysis of the absorbance vs. ligand concentration data at 422 nm. Similar results were obtained for the data at 407 nm.

To ascertain the specific interaction of the nitrogenous base with the Fe porphyrin, titration experiments were carried out and the progress of the reaction was monitored spectrophotometrically. Figure 3 depicts the spectra obtained over the Soret region as microliter volumes of a 1.24×10^{-2} M pyridine solution were incrementally added to a 2.34×10^{-6} M (TPP)FeCS solution. The clean isosbestic points at 414 nm indicated a neat (TPP)FeCS to (TPP)FeCS[py] conversion with no long-lived intermediates and no decomposition of product. Analysis of the data by the method of Benesi and Hildebrand (see the inset of Figure 3) indicated that 0.97 pyridine molecule were involved in the complexation reaction. Similar results were obtained for all 15 nitrogeneous bases listed in Table I. Titrations for each nitrogeneous base utilized were carried out in triplicate.

IR spectroscopy was utilized to ensure retention of the thiocarbonyl moiety during the complexation with the nitrogenous bases. In both $EtCl_2$ and $CHCl_3$, the C=S stretching frequency for (TPP)FeCS was 1308 cm^{-1}. This value was comparable to the value of 1310 cm^{-1} reported by Mansuy and

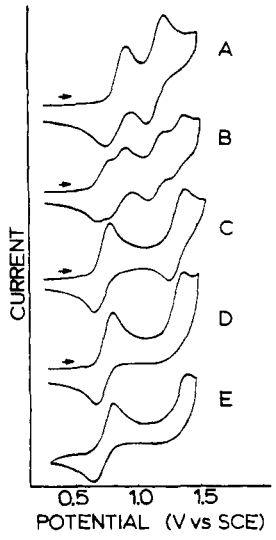

Figure 4. Cyclic voltammograms obtained during the electrooxidation of (TPP)FeCS dissolved in $EtCl_2$ containing 0.1 M TBAP and various amounts of 3-picoline: (A) 0.0 equiv; (B) 0.5 equiv; (C) 1.0 equiv; (D) 1.4 equiv. Traces A–D were first scan cyclic voltammograms. Trace E is the steady-state voltammogram obtained after five continuous potential scans. All voltammograms were obtained at a potential sweep rate of 100 mV s^{-1}.

co-workers[9] for (TPP)FeCS confined in a KBr pellet. Addition of nitrogeneous bases to (TPP)FeCS/$CHCl_3$ solutions shifted the C=S stretching frequency to lower energies. The specific values for the C=S stretch are also listed in Table I.

Voltammetric Characterization of (TPP)FeCS[L] Complexes. Two separate electron-transfer processes were observed during the electrooxidation of (TPP)FeCS[L] complexes in $EtCl_2$ solution. Typical cyclic voltammograms are depicted in Figure 4b–e for electrooxidation of (TPP)FeCS complexed with 3-picoline. At less than 1 equiv of 3-picoline (Figure 4b), four separate electron transfers are observed; the processes at $E_{1/2}$ = 0.85 and 1.16 V correspond to the oxidation of the uncomplexed Fe porphyrin whereas the other two processes at $E_{1/2}$ = 0.72 and 1.30 V correspond to the sequential oxidation of the complexed Fe porphyrin. Increasing the concentration of 3-picoline to 1 equiv (Figure 4c) yields a cyclic voltammogram with only two processes, indicating that the complexation reactions are complete. In the presence of an excess of 3-picoline, the first oxidation step remains chemically reversible whereas the second step is rendered chemically irreversible by a fast chemical reaction following the electron-transfer step. Analysis of the cyclic voltammetric data obtained for the first oxidation process over the potential sweep range of 10–500 mV s^{-1} indicated that the half-wave potential (measured at 718 ± 5 mV) was independent of potential sweep rate. The cathodic to anodic peak current ratio was equal to 1 and independent of potential sweep rate. The ratio of the anodic peak current over the square root of the potential sweep rate was a constant value for all measurements. At a potential sweep rate of 10 mV s^{-1}, the anodic to cathodic peak potential separation was 63 ± 1 mV and increased with increasing potential sweep. At the same potential sweep rate, the difference between the anodic peak potential and the potential at half the anodic peak current was 60 ± 1 mV and also increased with increasing sweep rate. These data indicated that the first oxidation of (TPP)FeCS[3-pic] (3-pic = 3-picoline) is best described as a reversible, one-electron transfer.

At 1 equiv of ligand, the second oxidation process exhibited voltammetric characteristics similar to those described above for the first oxidation process. However, in the presence of excess ligand concentration, the ratio of the peak currents became dependent upon the concentration of ligand present as well as the rate of potential sweep (see Figure 4d). The anodic peak geometry ($E_{p,a} - E_{p,a/2}$) indicated that a one-electron-transfer process was maintained. The anodic peak potential shifted cathodically by ~50 mV per decade of potential sweep rate. These results confirmed that (1) the second oxidation step is best described as a reversible electron transfer with a fast chemical reaction following the electron-transfer step and (2) the rate of the chemical reaction was proportional to the concentration of excess ligand present in solution. The steady-state voltammogram, depicted in Figure 4e, indicated that the product of the following chemical reaction is readily converted back to (TPP)FeCS[3-pic] via a one-electron reduction. At ligand to porphyrin ratios greater than 1.4, a third process at E_p = 1.48 V, characteristic of the irreversible oxidation of the free ligand, was observed.

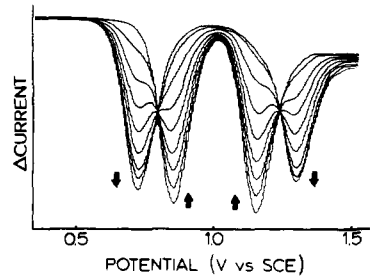

Figure 5. Differential-pulse voltammetry data obtained during the titration of (TPP)FeCS with 3-picoline. The pertinent instrumental parameters were a potential sweep rate of 10 mV s^{-1}, a pulse interval of 0.5 s, and a pulse amplitude of 25 mV. The scan depicted were taken over the 3-picoline concentration range of 0.0–1.1 equiv.

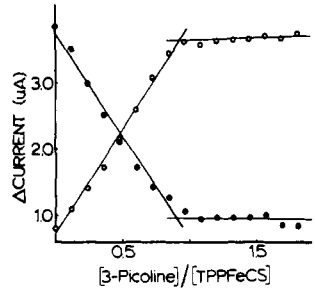

Figure 6. Plot of the change in peak current as a function of the molar ratio of 3-picoline to (TPP)FeCS. Open circles denote the decrease in peak current for the oxidation of the uncomplexed species, (TPP)FeCS (E_p = 0.86 V in Figure 5), whereas the closed circles denote the increase in peak current for the oxidation of the complexed material (TPP)FeCS[3-pic] (E_p = 0.73 V in Figure 5).

Similar results were obtained for all of the nitrogenous bases investigated. Comparison of the cyclic voltammograms obtained in the presence of excess ligand indicated that the rate of the chemical reaction following the second oxidation step increased with increasing basicity of the ligand.

To ascertain the specific interaction of the nitrogenous base with the oxidized forms of the Fe porphyrin, differential-pulse voltammetric experiments were carried out during the titration of (TPP)FeCS with the nitrogenous bases. Figure 5 depicts the data obtained during the titration of (TPP)FeCS with 3-picoline. In the absence of ligand, the two oxidation processes corresponding to the oxidation of the unligated complex were observed at E_p = 0.86 and 1.17 V, respectively. Incremental additions of aliquots of ligand resulted in a decrease in both peak curents while new processes made their appearance at 0.73 and 1.31 V, respectively. Note that there is no shift in the peak potentials with increasing ligand concentration. This finding indicated that the number of ligands coordinating with (TPP)FeCS is identical with the number of ligands coordinating with both of the oxidized materials. A plot depicting the peak current for each of the processes

Table II. Potential Data[a] for Oxidation of (TPP)FeCS[L] Adducts

ligand	pK_{BH^+}[b]	substituent const[c]	$E_{1/2}$, V 1st oxidn	$E_{1/2}$, V 2nd oxidn
none			0.85	1.16
3,5-dichloropyridine	0.67	0.74	0.83	1.28
3-cyanopyridine	1.45	0.68	0.81	1.30
4-cyanopyridine	1.85	0.66	0.80	1.29
3-chloropyridine	2.81	0.37	0.78	1.30
3-bromopyridine	2.84	0.39	0.78	1.31
3-acetylpyridine	3.18	0.38		
4-acetylpyridine	3.51	0.22	0.76	1.29
aniline	4.63			
pyridine	5.28	0.00	0.73	1.27
3-picoline	5.77	−0.07	0.72	1.30
4-picoline	5.98	−0.17	0.71	1.29
3,4-dimethylpyridine	6.46	−0.24	0.71	1.30
imidazole	6.65		0.65	1.22

[a] Measured at 23 ± 2 °C in 0.1 M TBAP/$EtCl_2$. [b] Values taken from: Schoefield, K. S. "Hetero-Aromatic Nitrogen Compounds"; Plenum Press: New York, 1967; p 146. [c] Values taken from: Jaffe, H. H. *Chem. Rev.* 1953, *53*, 191.

shown in Figure 5 vs. the molar ratio of ligand to porphyrin concentrations is depicted in Figure 6. For the processes at E_p = 0.72 and 1.30 V, the peak currents increased linearly up to a [3-picoline]/[(TPP)FeCS] ratio of 1.0. Above this ratio, the peak currents were constant and were independent of ligand concentration. Likewise, the peak currents for processes located at E_p = 0.86 and 1.17 V decreased in a linear fashion with increasing ligand concentration. At ligand to porphyrin ratios larger than 1.2, both processes were no longer distinguishable from the background level. Both the peak potential and peak current magnitude for the first oxidation process were unaffected even up to a 1000-fold excess of ligand. Identical relationships between the peak current and the molar ratio of ligand to porphyrin were observed for the second oxidation process at concentration ratios less than 1.3. At higher concentration ratios, the process at 1.30 V became irreversible.

Similar results were obtained for the other nitrogenous bases utilized in this study. The half-wave potentials for the sequential oxidation of the (TPP)FeCS[L] complexes investigated are listed in Table II. These data, taken collectively, indicated that the starting material and both of its oxidation products coordinated one and only one nitrogenous base molecule.

Spectroelectrochemical Characterization of (TPP)FeCS[L] Complexes. An incremental potential-step experiment was performed on a solution of (TPP)FeCS containing a 2-fold excess of 3-picoline. The spectra recorded as the potential was stepped incrementally from 0.50 to 1.15 V are depicted in the upper portion of Figure 7. The first oxidation of (TPP)-FeCS[3-pic] produced a sizable decrease in intensity and a blue shift of 7 nm for the Soret band. The α and β bands shifted to 584 and 511 nm, respectively. Isosbestic points were observed at 411, 441, 534, and 555 nm during the course of the transformation from electrode reactant to product. Analysis of the spectral absorbance changes as a function of the applied potential confirmed the passage of 1 equiv of charge and a formal potential of 0.72 V for this oxidation process.

Holding the potential at 1.15 V for 3 h produced no spectral changes as a function of time. Returning the applied potential to 0.50 V yielded the spectrum characteristic of the starting material, (TPP)FeCS[3-pic], within 20 s. Evaluation of the Soret band intensities before and after the potential-step experiments indicated that 99% of the material was reversibly oxidized.

Similar results were obtained with the ligands listed in Table III. The salient features obtained during the spectral transition from electrode reactant to product, in both the presence and absence of ligand, are listed for comparison.

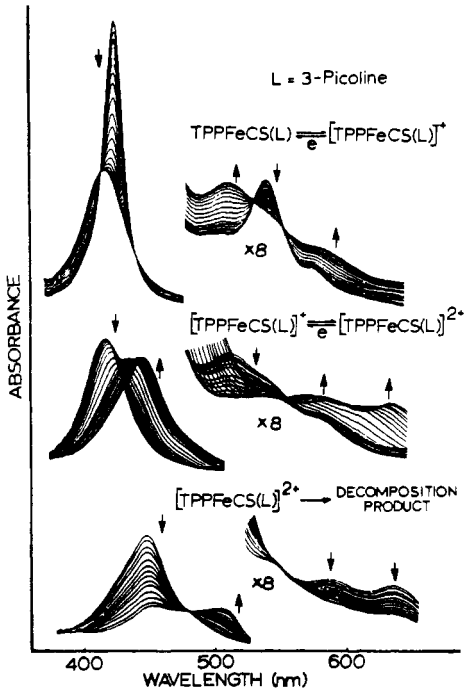

Figure 7. Spectra obtained during the incremental potential-step experiment on a solution of 0.292 mM (TPP)FeCS in $EtCl_2$ containing 0.1 M TBAP and 2 equiv of 3-picoline over the potential region 0.50–1.5 V (upper portion), 1.15–1.37 V (middle portion), and 1.37–1.55 V (lower portion).

Table III. Spectral Data Obtained during the Electrolysis of (TPP)FeCS[L] Adducts[a]

ligand	electronic spectral data[b] (TPP)Fe^{II}CS[L]	{(TPP)Fe^{III}CS[L]}+	isosbestic points
none	407 (1.92)	408 (0.91)	396, 424
	522 (0.14)	510 (0.14)	515, 536
	548 (0.08)	596 (0.08)	
3,5-dichloro-	421 (2.04)	413 (1.06)	410, 443
pyridine	541 (0.13)	513 (0.13)	536, 559
	577 (0.05)	588 (0.06)	
3-chloro-	421 (1.91)	410 (0.82)	410, 440
pyridine	542 (0.12)	514 (0.11)	536, 557
	578 (0.05)	591 (0.05)	
pyridine	422 (2.03)	415 (1.03)	413, 437
	542 (0.12)	517 (0.09)	532, 559
	579 (0.07)	587 (0.05)	
3-picoline	422 (1.89)	415 (0.92)	411, 441
	543 (0.09)	511 (0.08)	534, 555
	579 (0.04)	584 (0.06)	

[a] Solvent system: $EtCl_2$, 0.1 M in TBAP. [b] Values listed are peak peak maxima in nm; values in parentheses are the molar absorptivities at peak maximum divided by 10^5.

The spectra depicted in the middle and lower portions of Figure 7 were acquired 3.0 min after the application of the desired potential beyond 1.15 V. Sequential scanning experiments (not shown) at shorter delay times indicated that these spectra do not represent equilibrium concentrations of electrode reactant and product. Rather, these spectra are a composite of the electrode reactant, the initial product of the electron transfer, and the product of the chemical reaction that follows the electron transfer.

Time-resolved thin-layer spectroelectrochemical experiments carried out on a fresh solution of (TPP)FeCS containing 3 equiv of 3-picoline produced similar results. Stepping the potential from 0.50 to 1.15 V yielded spectra characteristic of the one-electron-oxidized species, {(TPP)FeCS[3-pic]}+.

Scheme I

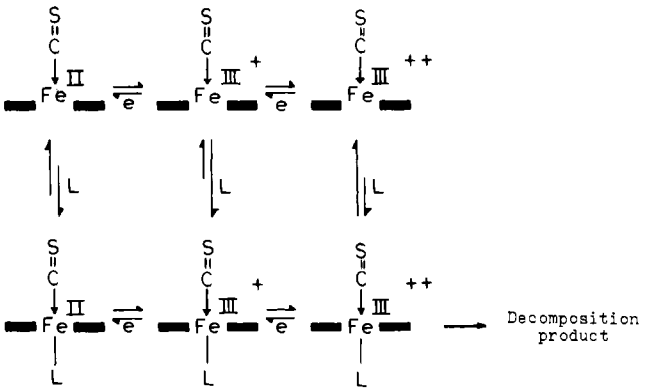

Stepping the potential to 1.42 V and monitoring the spectra at 5-s intervals yielded a smooth transition between the Soret band of the cation (at 415 nm) to one at 446 nm with an isosbestic point at 423 nm, only for the first six spectral acquisitions (30 s after the onset of the potential). At longer times, the spectral transition proceeded in a similar fashion to that depicted in the middle and lower portions of Figure 7. Reversing the potential to 1.15 V did not regenerate the spectrum assigned to either $\{(TPP)FeCS[3\text{-pic}]\}^+$ or $\{(TPP)Fe[3\text{-pic}]_2\}^+$. Reducing the ligand concentration to exactly 1 equiv did not eliminate the chemical decomposition to $\{(TPP)FeCS[3\text{-pic}]\}^{2+}$ but did significantly extend the lifetime of this intermediate species. Interestingly, after formation of the material whose spectrum is given in the final spectra of Figure 7 (lower portion), returning the electrode potential to 0.50 V did not regenerate the spectrum of the starting material, (TPP)FeCS[3-pic]. This finding contrasts with the results of the steady-state voltammetric data depicted in Figure 4e.

Similar results were obtained when 3,5-dichloropyridine, 3-chloropyridine, and pyridine were utilized as axial ligands. In all cases, the rate of the chemical reaction was proportional to both the concentration of free ligand in solution as well as the basicity of the ligand utilized.

Discussion

Electrode Mechanism for Oxidation of (TPP)FeCS. Taken collectively, the voltammetric results indicated that the electrooxidation of (TPP)FeCS proceeded in two discrete, single-electron, quasi-reversible steps, as shown in the upper portion of Scheme I. The product of the first electron transfer is assigned as a thiocarbonyl Fe(III) porphyrin for the following reasons. First, the spectral interconversion between the starting material and the first oxidation product was chemically reversible and characterized by well-defined isosbestic points. The electronic spectrum of the product possessed features characteristic of Fe(III) porphyrins, i.e. diminished Soret band intensity (as compared to the Fe(II) starting material) and an increase in separation between the α and β bands.[27] Second, the IR stretch characteristic of (TPP)Fe cation radicals[28] was not present in the spectrum taken on oxidized material. Third, the EPR spectrum of the product of the first electrooxidation step was consistent with that expected for a low-spin Fe(III) porphyrin.[29] Finally, the IR vibration previously assigned to the C=S stretch (at 1308 cm^{-1}) shifted to 1374 cm^{-1} upon oxidation. This is consistent with expectations for coordination of the C=S moiety to a more electropositive metal center. The Fe(III) assignment also concurs with that previously put forth by Buchler and co-workers[11] for oxidation of (OEP)FeCS.

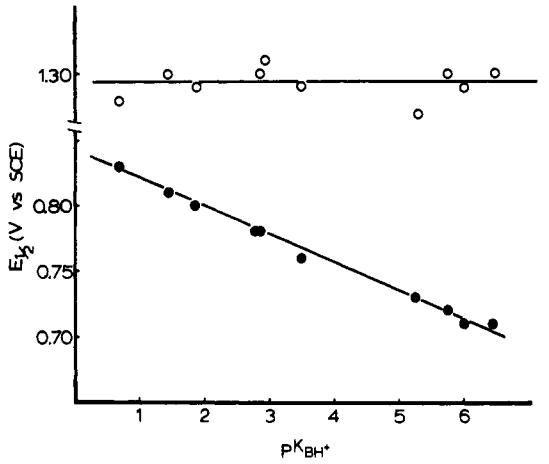

Figure 8. Plot of the half-wave potential data for oxidation of (TPP)FeCS[L] complexes vs. the basicity of the nitrogenous base ligand. Closed circles denote the first oxidation process while the open circles denote the second oxidation process.

The product of the second oxidation step is formally assigned as a thiocarbonyl Fe(III) porphyrin cation radical. This assignment is based on the following observations. First, the electronic spectrum is comparable to that previously observed for porphyrin cation radicals.[30] Second, the potential separation between the second oxidation process and that of the first reduction process is within the limits previously established for the ring-centered electron-transfer reactions of metalloporphyrins.[31] Lexa and co-workers[13,14] have previously assigned the reduction process at −1.31 V to the formation of the (TPP)FeCS porphyrin radical anion. Third, the chemical reversibility of the second oxidation reaction (greater than 97%) during the spectroelectrochemical experiments as well as the absence of the chemistry expected for free :C=S strongly infers retention of the thiocarbonyl moiety on the Fe(III) porphyrin cation radical.

Electrode Mechanism for Oxidation of (TPP)FeCS(L) Complexes. The electron-transfer pathway for electrooxidation of (TPP)FeCS(L) is shown in the lower portion of Scheme I. The first oxidation of (TPP)FeCS(L) yields a six-coordinate, unsymmetrically substituted thiocarbonyl Fe(III) porphyrin. This assignment concurs with that previously put forth by Buchler and co-workers[11] for (OEP)FeCSpy. The rationale behind this assignment follows the lines presented above.

Previous investigations on the oxidative chemistry of six-coordinate Fe porphyrins have indicated that the half-wave potential can be an indicator of the ultimate site of electron transfer. Bottomley and Kadish[32] have shown that the oxidation potentials for six-coordinate Fe(II) porphyrins varied linearly with the pK_{BH^+} of the axial ligand. These workers, as well as Goff and co-workers[33] have demonstrated that the potential for oxidation of the porphyrin ring is independent of the basicity of the Fe center's axial ligand. A plot of the half-wave potential measured for both the first and second

(27) (a) Felton, R. H. In "The Porphyrins"; Dolphin, D., Ed.; Academic Press: New York, 1979; Vol. V, Chapter 3. (b) Walker, F. A.; Lo, M.-W.; Ree, M. T. *J. Am. Chem. Soc.* **1976**, *98*, 5552.
(28) Shimomura, E. T.; Phillippi, M. A.; Goff, H. M.; Scholz, W. F.; Reed, C. A. *J. Am. Chem. Soc.* **1981**, *103*, 6778.
(29) Palmer, G. In "Iron Porphyrins"; Lever, A. B. P., Gray, H. B., Jr., Eds.; Addison-Wesley: Reading, MA, 1983; Part II, Chapter 2.
(30) (a) Carnieri, N.; Harriman, A. *Inorg. Chim. Acta* **1982**, *62*, 103. (b) Wollberg, A.; Manassen, J. *J. Am. Chem. Soc.* **1970**, *92*, 2982. (c) Gans, P.; Marchon, J. C.; Reed, C. A.; Regnard, J. R. *Nouv. J. Chim.* **1981**, *5*, 203.
(31) Fuhrhop, J. H.; Kadish, K. M.; Davis, D. G. *J. Am. Chem. Soc.* **1973**, *95*, 5140.
(32) (a) Bottomley, L. A.; Kadish, K. M. *Inorg. Chem.* **1981**, *20*, 1348. (b) Kadish, K. M.; Bottomley, L. A. *Ibid.* **1980**, *19*, 832.
(33) (a) Phillippi, M. A.; Shimomura, E. T.; Goff, H. M. *Inorg. Chem.* **1981**, *20*, 1322. (b) Phillippi, M. A.; Goff, H. M. *J. Am. Chem. Soc.* **1982**, *104*, 6026.

Table IV. Formation Constants[a] for (TPP)FeCS[L] Adducts

ligand	pK_{BH^+}[b]	substituent const[c]	log B^0	log B^+ [d]	log B^{2+} [e]
3,5-dichloropyridine	0.67	0.74	2.90 ± 0.05	3.2	1.1
3-cyanopyridine	1.45	0.68	3.06 ± 0.02	3.7	1.3
4-cyanopyridine	1.85	0.66	3.20 ± 0.03	4.2	2.0
3-chloropyridine	2.81	0.37	3.23 ± 0.04	4.4	1.9
3-bromopyridine	2.84	0.39	3.43 ± 0.04	4.7	2.1
3-acetylpyridine	3.18	0.38	4.19 ± 0.02		
4-acetylpyridine	3.51	0.22	3.88 ± 0.05	5.4	3.2
aniline	4.63		3.57 ± 0.01		
pyridine	5.28	0.00	3.92 ± 0.03	6.2	4.3
3-picoline	5.77	−0.07	4.10 ± 0.02	6.2	3.9
4-picoline	5.98	−0.17	4.34 ± 0.02	6.7	4.5
3,4-dimethylpyridine	6.46	−0.24	4.63 ± 0.08	7.0	4.6
imidazole	6.65		4.99 ± 0.06	8.4	7.4
methylimidazole	7.33		5.23 ± 0.03		
piperidine	11.10		6.00 ± 0.06		

[a] Measured at 23 ± 2 °C in 0.1 M TBAP/$EtCl_2$. [b] Values taken from: Schoefield, K. S. "Hetero-Atomatic Nitrogen Compounds"; Plenum Press: New York, 1967; p 146. [c] Values taken from: Jaffe, H. H. *Chem. Rev.* **1953**, *53*, 191. [d] Uncertainties are ±0.2 log unit. [e] Uncertainties are ±0.3 log unit.

oxidation steps vs. the pK_{BH^+} is depicted in Figure 8. The assignment of the first oxidation as a metal-centered electron transfer is confirmed by the linear relationship obtained. Similarly, the independence of the second oxidation potential on the basicity of the axial ligand is in strong support of the Fe(III) porphyrin cation radical assignment.

The nature of the $\{(TPP)Fe^{III}CS[L]\}^{2+}$ decomposition reaction(s) is of interest. The cyclic voltammetric data presented in Figure 4 manifest the electrochemical reversibility of the $\{(TPP)Fe^{III}CS[L]\}^{+}$ to $\{(TPP)Fe^{III}CS[L]\}^{2+}$ step in the absence of an excess of nitrogenous base. In the presence of an excess of ligand, the lifetime of the dication at the electrode is drastically reduced. The qualitative relationship between the concentration of excess ligand present and the decrease in the lifetime of the dication infers that the nitrogenous base plays an integral part in the chemical reaction following the electron transfer. Nucleophilic attack on porphyrin cation radicals have been well substantiated in the literature.[34] However, the actual mechanism is not well understood.[35] Kadish and Rhodes[35] have observed cyclic voltammetric and spectroelectrochemical results for the electrooxidation of (TPP)Zn[L] complexes very similar to the results presented herein. Analysis of the final spectrum in Figure 7 indicated that the product of the decomposition reaction possesses a split Soret with peaks at 454 and 508 nm. This is indicative of an interruption in the conjugation of the porphyrin π system, most likely due to the formation of a nitrogenous base–isoporphyrin dication derivative.

Formation Constants for Ligand Addition. On the basis of absorbance changes as a function of ligand concentration,[21] formation constants (as defined in eq 1) for addition of one

$$B^0 = [(TPP)Fe^{II}CS[L]]/[(TPP)Fe^{II}CS][L] \quad (1)$$

nitrogenous base to (TPP)FeCS were computed. The values obtained for the nitrogenous bases utilized are listed in Table IV. Formation constants (as defined in eq 2 and 3) for

$$B^+ = [\{(TPP)Fe^{III}CS[L]\}^+]/[\{(TPP)Fe^{III}CS\}^+][L] \quad (2)$$

$$B^{2+} = [\{(TPP)Fe^{III}CS(L)\}^{2+}]/[\{(TPP)Fe^{III}CS\}^{2+}][L] \quad (3)$$

addition of one nitrogenous base to the Fe(III) and Fe(III) porphyrin cation radical were computed from the half-wave potential data in the usual fashion[23] and are also listed in Table IV. To our knowledge, the values reported as log B^{2+} represent the first formation constants measured for ligand addition to Fe porphyrin cation radicals.

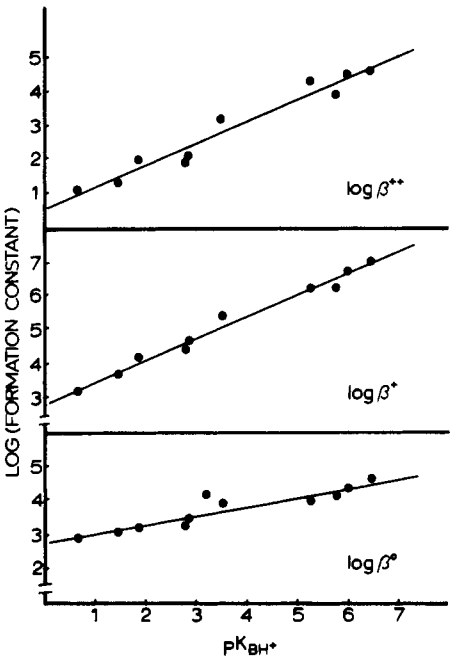

Figure 9. Correlation between the logarithm of the formation constants for $(TPP)Fe^{II}CS[L]$ (lower), $\{(TPP)Fe^{III}CS[L]\}^+$ (middle), and $\{TPPFe^{III}CS[L]\}^{2+}$ (top) vs. the basicity of the nitrogenous base utilized as the axial ligand.

A large number of linear free energy relationships have been presented in the literature for ligand-addition reactions of metalloporphyrins. Plots of the logarithm of the formation constant vs. pK_{BH^+} of the axial base for a series of closely related ligands are used to evaluate whether the σ or π bonding mode predominates in the ligand to metal interaction. In this context, a plot of the logarithm of the formation constants for the three species observed in the study vs. the pK_{BH^+} of the axial ligand is depicted in Figure 9. Linear relationships were obtained throughout. Slope magnitudes of 0.27, 0.63, and 0.64 were computed from linear least-squares analysis of log B^0, log B^+, and log B^{2+}, respectively. The formation constants for addition of the imidazoles were not included in this fit as their magnitudes were consistently higher than observed for the pyridines of comparable pK_{BH^+}. This observation, coupled with the observed linear relationship and the fit of the nonaromatic amines on the trace, suggests that σ bonding predominates the nitrogenous base to Fe interaction for all three thiocarbonyl

(34) Shine, H. J.; Padilla, A. G.; Wu, S.-M. *J. Org. Chem.* **1979**, *44*, 4069.
(35) Kadish, K. M.; Rhodes, R. K. *Inorg. Chem.* **1981**, *20*, 2961.

Fe porphyrin species. Linear relationships were also obtained when the logarithm of the formation constants were plotted vs. the Hammett-Taft substituent constant for each substituted pyridine.

Battioni et al.[9] have shown that the C=S stretching frequency for (TPP)FeCS[L] complexes (measured in a KBr pellet) was dependent upon the identity of L. Buchler and co-workers[36] have previously investigated trans effects on the mixed CO-L complexes for Fe, Ru, and Os porphyrins. They observed that the trans effects in the C=O stretching frequencies were explicable by the basicity of the ligand trans to C=O in the case of Fe. However, this explanation was not applicable to Os porphyrins, in which both σ and π donor and acceptor properties had to be considered.

The results presented in Table I concur with the findings of both Battioni and Buchler. A linear relationship between the C=S stretching frequency and the pK_{BH^+} of the ligand trans to the C=S moiety was obtained and is consistent with expectations. The ligand series of substituted pyridines was selected to provide a means for evaluating the trans effect operative in the (TPP)FeCS[L] system over the widest range of pK_{BH^+} values available. The C=S stretching frequency decreased as the π donor ability of the Fe center increased. The pK_{BH^+} of the amine trans to the C=S moiety is a measure of the amine to Fe σ interaction and, by induction, controls the π donor ability of the Fe center.

The observation of two chemically reversible oxidations for the thiocarbonyl Fe(II) porphyrin is particularly intriguing when compared with the analogous carbon monoxide adducts of Fe(II) porphyrins. Brown et al.[15] reported that (Etio)FeCO(ImH) was irreversibly oxidized at $E_p = 0.32$ V in CH_2Cl_2. Buchler and co-workers[11] observed similar behavior for (OEP)FeCOpy at $E_p = 0.43$ V. Gurira and Jordan[16] have investigated the oxidation of (protoporphyrin IX)$Fe^{II}CO$ in aqueous media. In all cases reported to date, oxidation of the carbon monoxide bound Fe(II) porphyrin proceeds concomitantly with the loss of CO. In nonaqueous media, the dissociation appears to occur very rapidly after the electron transfer.[37] These observations are in marked contrast with the behavior of the thiocarbonyl Fe porphyrins. Scheidt and Geiger[38] have utilized (OEP)FeCS as a stereochemical equivalent for the analogous five-coordinate complex (OEP)FeCO. Clearly, this analogy does not extend to either the redox or coordination chemistry of these two carbene Fe porphyrin complexes.

Acknowledgment is made to the donors of the Petroleum Research Fund, administered by the American Chemical Society, and to the Cottrell Grants Program of the Research Corp. for support of this research.

Registry No. (TPP)FeCS, 67583-11-3; $\{(TPP)FeCS\}^+$, 92054-41-6; $\{(TPP)FeCS\}^{2+}$, 92054-46-1; (TPP)FeCS[L] (L = 3,5-dichloropyridine), 92054-29-0; $\{(TPP)FeCS[L]\}^+$ (L = 3,5-dichloropyridine), 92054-42-7; $\{(TPP)FeCS[L]\}^{2+}$ (L = 3,5-dichloropyridine), 92054-55-2; (TPP)FeCS[L] (L = 3-cyanopyridine), 92054-30-3; $\{(TPP)FeCS[L]\}^+$ (L = 3-cyanopyridine), 92054-48-3; $\{(TPP)FeCS[L]\}^{2+}$ (L = 3-cyanopyridine), 92054-56-3; (TPP)FeCS[L] (L = 4-cyanopyridine), 92054-31-4; $\{(TPP)FeCS[L]\}^+$ (L = 4-cyanopyridine), 92054-49-4; $\{(TPP)FeCS[L]\}^{2+}$ (L = 4-cyanopyridine), 92054-57-4; (TPP)FeCS[L] (L = 3-chloropyridine), 92054-32-5; $\{(TPP)FeCS[L]\}^+$ (L = 3-chloropyridine), 92054-43-8; $\{(TPP)FeCS[L]\}^{2+}$ (L = 3-chloropyridine), 92054-58-5; (TPP)FeCS[L] (L = 3-bromopyridine), 92054-33-6; $\{(TPP)FeCS[L]\}^+$ (L = 3-bromopyridine), 92054-50-7; $\{(TPP)FeCS[L]\}^{2+}$ (L = 3-bromopyridine), 92054-59-6; (TPP)FeCS[L] (L = 3-acetylpyridine), 92054-34-7; (TPP)FeCS[L] (L = 4-acetylpyridine), 92054-35-8; $\{(TPP)FeCS[L]\}^+$ (L = 4-acetylpyridine), 92054-51-8; $\{(TPP)FeCS[L]\}^{2+}$ (L = 4-acetylpyridine), 92054-60-9; (TPP)FeCS[py], 67670-43-3; $\{(TPP)FeCS[py]\}^+$, 92054-44-9; $\{(TPP)FeCS[py]\}^{2+}$, 92054-61-0; (TPP)FeCS[3-pic], 92054-37-0; $\{(TPP)FeCS[3\text{-}pic]\}^+$, 92054-45-0; $\{(TPP)FeCS[3\text{-}pic]\}^{2+}$, 92054-47-2; (TPP)FeCS[4-pic], 92054-38-1; $\{(TPP)FeCS[4\text{-}pic]\}^+$, 92054-52-9; $\{(TPP)FeCS[4\text{-}pic]\}^{2+}$, 92054-62-1; (TPP)FeCS[L] (L = 3,4-dimethylpyridine), 92054-39-2; $\{(TPP)FeCS[L]\}^+$ (L = 3,4-dimethylpyridine), 92054-53-0; $\{(TPP)FeCS[L]\}^{2+}$ (L = 3,4-dimethylpyridine), 92054-63-2; (TPP)FeCS[L] (L = imidazole), 92054-40-5; $\{(TPP)FeCS[L]\}^+$ (L = imidazole), 92054-54-1; $\{(TPP)FeCS[L]\}^{2+}$ (L = imidazole), 92054-64-3; (TPP)FeCS[L] (L = methylimidazole), 80697-79-6; (TPP)FeCS[L] (L = piperidine), 92078-13-2; (TPP)FeCS[L] (L = aniline), 92054-36-9.

(36) Buchler, J. W.; Kokisch, W.; Smith, P. D. *Struct. Bonding (Berlin)* **1980**, *34*, 79.

(37) During the course of cyclic voltammetric experiments conducted at low temperature, an increase in the reversibility of the electrooxidation of (TPP)FeCO has been observed: Kadish, K. M., private communication.

(38) Scheidt, W. R.; Geiger, D. K. *Inorg. Chem.* **1982**, *21*, 1208.

Contribution from the Department of Chemistry, University of Technology, Loughborough, Leicestershire, United Kingdom

Quenching of the Triplet States of Organic Compounds by Iron(III) Complexes of β-Diketones due to Reversible Electron Transfer

F. WILKINSON* and C. TSIAMIS

Received January 5, 1984

The rate constants, k_q, for quenching of the triplet states of 15 different organic molecules by iron(III) tris(1,1,1-trifluoro-2,4-pentanedionate), $Fe(tfac)_3$, and by iron(III) tris(1,1,1,5,5,5-hexafluoro-2,4-pentanedionate), $Fe(hfac)_3$, in benzene solution have been measured by using the technique of nanosecond laser flash photolysis. Limiting high k_q values of $(6.3 \pm 0.2) \times 10^9$ and $(7.9 \pm 0.2) \times 10^9$ dm^3 mol^{-1} s^{-1} were obtained for quenching of several triplet states by $Fe(tfac)_3$ and $Fe(hfac)_3$, respectively. The quenching efficiencies are compared with those of $Fe(acac)_3$, which has been previously shown to quench by the mechanism of electronic energy transfer, and the marked increase in the efficiency of quenching especially for low-energy triplet donors by these iron(III) complexes containing the fluorinated ligands is shown to be due to the occurrence of the additional mechanism of reversible electron-transfer quenching. Correlations of the quenching rate constants with the standard Gibbs free energy change for electron transfer to the iron(III) complexes allow an intrinsic barrier of 0.26 eV for both quenchers and transmission coefficients of 0.007 and 0.014 to be evaluated for electron transfer from electronically excited triplet states to $Fe(tfac)_3$ and $Fe(hfac)_3$, respectively.

Introduction

The photochemistry and photophysics of coordination compounds is a topic of current interest. Information concerning excited states obtainable from absorption and emission spectra can be greatly amplified and extended by making sensitization and quenching studies. In fluid solution, transition-metal

0020-1669/84/1323-3571$01.50/0